Desalination and Water Treatment
www.deswater.com

doi: 10.1080/19443994.2014.968630

56 (2015) 3346–3356
December

Taylor & Francis
Taylor & Francis Group

Degradation of burazol blue ED by heterogeneous fenton process: simultaneous optimization by central composite design

Umut Akay, Ezgi Aktar Demirtas*

Department of Industrial Engineering; Eskisehir Osmangazi University, Eskisehir 26040, Turkey, emails: akayumut@gmail.com (U. Akay), eaktar@ogu.edu.tr (E.A. Demirtas)

Received 28 February 2014; Accepted 14 September 2014

ABSTRACT

This work is an application of the response surface methodology (RSM) to determine the effects of operational parameters on the heterogeneous Fenton-type oxidation of the burazol blue ED (BB). The study was conducted using a Fe (III) sepiolite catalyst in the presence of hydrogen peroxide (H_2O_2) in a batch process. The effects of operational parameters such as the pH of the reaction, catalyst concentration, stirring speed, and reaction time were examined under the following conditions: a temperature of 25˚C, 100 ppm initial dye concentration, and 0.5 mM H_2O_2 concentration. Because of the significant curvature effect, central composite design (CCD) was preferred to full-factorial experimental design for the simultaneous optimization of color and chemical oxygen demand (COD) removals. Optimized reaction conditions were established as pH 2, 1 g/250 mL catalyst dose, 250-rpm stirring speed, and 60-min reaction time. Contour plots and a desirability function were used to find the local points of optimization. After conformation, under the optimized reaction conditions, 96% color and 75% COD removals were obtained experimentally. These values were in the prediction interval and were in agreement with the quadratic polynomial model predictions.

Keywords: Central composite design; Heterogeneous Fenton process; Color removal; COD removal; burazol blue ED

1. Introduction

Different industries such as textiles, dyeing, food, and printing use synthetic dyes extensively that belong to different dye families, such as azo, nitro, and indigo. Textile industry especially has shown a significant increase in the use of synthetic, complex organic dyes. The resulting colored wastewaters from the textile industry contain organic and inorganic chemicals that can be characterized by the high concentrations of COD and color that leads to serious pollution and disturbs the ecological balance. Dyes prevent transmittance of the sun light entering waterways by absorbing this light. Where this absorbance occurs, colored wastewaters can exhibit toxic effects on microbiological living beings by preventing the growth and photosynthetic activity of bacteria living in the water and can also create carcinogenic and toxic effects for other creatures. Additionally, color will likely be a discharging standard in the future. Therefore, treatment of wastewaters containing dyes before discharging them to the environment will become crucial. Treatment of azo dyes such as BB is difficult due to the complex molecular structure. Traditional treatment methods containing biochemical and coagulation

---

*Corresponding author.

processes are either costly, inefficient, or result in the production of secondary toxic wastewater [1].

In recent years, advanced oxidation processes are gaining attention. UV/oxidation technologies use oxidizing agents such as hydrogen peroxide and ozone, semiconductors such as titanium dioxide and zinc oxide in combination with UV light and the Fenton process. Iron salts and hydrogen peroxide are used together along with the advanced oxidation technologies currently used for dyestuff removal. Among these methods, the homogeneous Fenton/photo-Fenton process deserves considerable attention. The homogeneous Fenton process uses low concentrations of Fe and H_2O_2 reagents to produce OH radicals with a high oxidation potential.

Fenton reaction involves several reactions, which can be described by Eqs. (1–4) by Martinez et al. [2]:

$$\mathrm{Fe^{3+} + H_2O_2 \rightarrow Fe(OOH)^{+2} + H^+} \tag{1}$$

$$\mathrm{Fe(OOH)^{+2} \rightarrow Fe^{+2} + HO_2\boldsymbol{.}} \tag{2}$$

$$\mathrm{Fe^{+2} + H_2O_2 \rightarrow Fe^{+3} + OH\boldsymbol{.} + OH} \tag{3}$$

$$\mathrm{Fe^{+3} + HO_2. \rightarrow Fe^{+2} + H^+ + O_2} \tag{4}$$

Although the homogeneous Fenton process is highly effective for removing organic compounds, the resulting necessity of iron salts removal from the wastewater is a great disadvantage of this method. In recent years, heterogeneous catalysts have taken the place of traditional homogeneous catalysts to overcome this drawback. Among these catalysts, zeolite, clay, activated carbon, and alumina are widely used for the color removal. Unlike other clays, sepiolite is gaining considerable attention because of its sorptive, rheologic, and catalytic properties, as well as its needle-like morphology. Moreover, the relatively low cost of sepiolite guarantees its continued utilization in the future [3].

Experimental design and RSM, which are superior in terms of time and cost while reducing the number of experiments, needed, unlike the classical trial-and-error method, have been applied to model and optimize different wastewater treatment processes. It is possible to estimate linear, interaction, and high-order (quadratic, cubic) effects of the input parameters and to establish a mathematical model for the prediction of the response by RSM [4].

CCD [4–8], Box–Behnken design [9–13], and constrained designs such as D-optimal [14] are different design types widely used in Fenton-type oxidation for the optimization of color, COD, or total organic carbon (TOC) removals. The differences between these designs include the number of runs required and the combinations of the levels used in the experiments. CCD gives almost as much information as a multilevel factorial and requires fewer experiments than full-factorial design.

In this study, CCD was used for the optimization of color and COD removals. The usage of Fe (III) sepiolite clay as a heterogeneous Fenton catalyst for the decolorization of BB was also examined. BB was selected as the modeled pollutant because of its unknown removal behavior in the literature. The effects of operational parameters, such as the pH (*A*) of the reaction, catalyst concentration (*B*), stirring speed (*C*), and reaction time (*D*), were examined under the following conditions: a temperature of 25˚C, 100 ppm initial dye concentration, and 0.5 mM H_2O_2 concentration. All factor levels were determined with respect to preliminary experiment results. Optimized reaction conditions were established as pH 2, 1 g/250 mL catalyst dose, 250-rpm stirring speed, and 60-min reaction time. Contour plots and a desirability function were used to find the local points of optimization. After conformation, under the optimized reaction conditions, 96% color and 75% COD removals were obtained experimentally. These values were in the prediction interval (PI) and were in agreement with the quadratic polynomial model predictions.

The main contribution of this paper is the optimization of two different responses (color and COD removals) simultaneously by using desirability functions. In general, responses such as color and TOC removals are optimized individually, but desirability functions provide a solution which enables a trade-off among two or more conflicting responses and used in RSM literature widely. However, the usage of desirability functions and simultaneous optimization was not encountered in the heterogeneous Fenton literature to the best of our knowledge.

2. Materials and methods

2.1. Materials and catalyst

The azo dye BB commonly used in textile industries was obtained from Burboya Co Textile Industry, Bursa, Turkey, at 45% purity and was used without further purification. The structure and characteristics of BB are presented in Table 1. Hydrogen peroxide (30%, w/w) and Fe $(NO_3)_3{\cdot}9H_2O$ were obtained from Sigma-Aldrich, Germany. All chemicals were analytical-grade reagents and were used as received without further purification. Deionized water was used, and the heterogeneous catalyst was the natural clay without

Table 1
Characteristics of RBB

Chemical structure	Molecular formula	Color	$\lambda_{\max\,(nm)}$	M_w (g/mol)
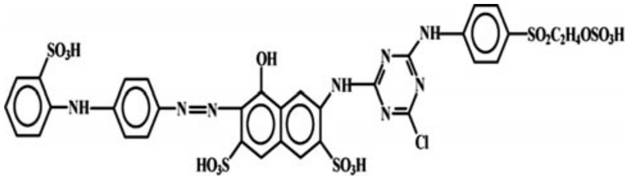	$C_{38}H_{41}N_8O_{16}S_5Cl$	Dark blue	594	1,061.54

pre-treatment, which was supplied from sepiolite mines in the Eskisehir region of Turkey. After washing and drying, the selected 0.038–0.053-mm-sized sepiolite was prepared through a cation exchange process as follows: 10 g sepiolite and 100 mL of 1 g/L $Fe(NO_3)_3{\cdot}9H_2O$ solution were mixed and shaken at 175 rpm for 6 h at 55˚C. The samples were washed with deionized water and dried at 105˚C. The characterization of this catalyst was done previously [3].

2.2. Experimental procedure

Chemical oxidation of BB was carried out in batch mode, using a beaker filled with 250 mL of the BB solution at a given concentration. In a typical run, the pH of the BB solution has been adjusted to the desired pH value by NaOH or H_2SO_4. After stabilization of the temperature and pH, the powder catalyst (Fe (III)-sepiolite) was added to the BB solution.

It was considered the beginning of the reaction when the required amount of H_2O_2 was added. All experiments were carried out under constant stirring to ensure good dispersion of the catalyst. Thereafter, samples were withdrawn periodically, centrifuged for 5 min to remove suspended particles, and analyzed using a UV–vis spectrophotometer (Shimadzu, model UV-120-01).

2.3. Analysis

Color removal was monitored by a UV–vis spectrophotometer at the $\lambda_{\max}$ value of 594 nm for BB. The color removal was determined using Eq. (5).

$$\%\,\text{Color removal} = \left(\frac{C_0 - C_t}{C_0}\right) \times 100 \tag{5}$$

where C_0 is the initial dye concentration in ppm and C_t is dye concentration at any time t. COD removal was measured at different time intervals by COD kits. The calculation of the extent of COD removal is shown in Eq. (6)

$$\%\,\text{COD removal} = \left(\frac{\text{COD}_0 - \text{COD}_t}{\text{COD}_0}\right) \times 100 \tag{6}$$

where COD_0 is the initial COD in ppm and COD_t is COD in ppm at any time t.

3. Results and discussion

3.1. Preliminary experiments

According to the results of studies in the literature, among all the variables, reaction time, temperature, catalyst dose, H_2O_2 concentration, stirring speed, and initial dye concentration have the largest influences on the heterogeneous Fenton-like decolorization [1–16].

Before experimental design and modeling, preliminary experiments were conducted following the single-factor method at each reaction time to decide the most influential operating parameters and their levels. The effect of pH was investigated in the range of 2–6. The results indicated that color and COD removals were significantly influenced by the pH of the solution.

Many studies reported in the literature have revealed that the use of higher concentration of Fe could lead to the self-scavenging of OH radical by Fe and induce the decrease in the degradation rate of pollutants [3]. In the present study, the suitable range of catalyst dosage was determined as 0–1.2 g/250 mL.

According to the results of preliminary experiments shown in Fig. 1, the optimum pH was 2.0 with 90% of color removal within 0.2 mg/250 mL catalyst concentration, 150-rpm stirring speed and 60-minute reaction time. At the same conditions, when the catalyst concentration was 1 mg/250 mL or stirring speed was 250 rpm, color removal has been reached to 92% approximately, On the other hand, maximum color

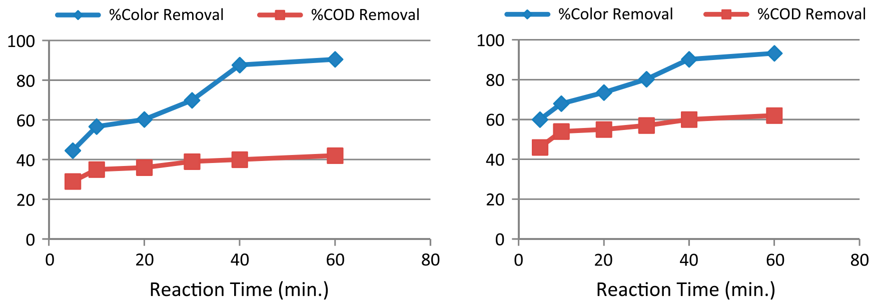

(a) A=2, B= 0.2g/250mL, C= 150 rpm

(b) A=2, B= 1g/250mL, C= 150 rpm

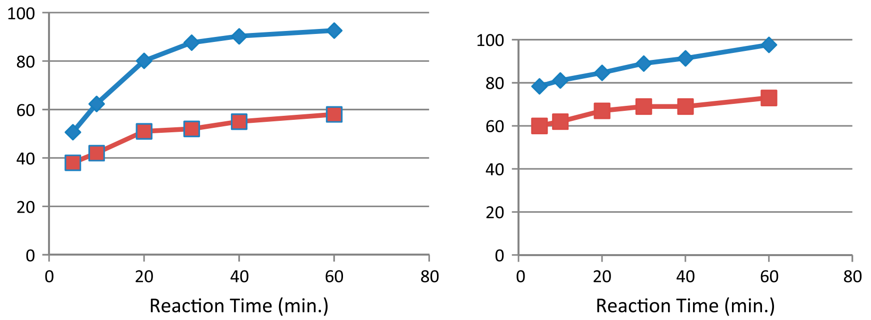

(c) A=2, B= 0.2 g/250mL, C= 250 rpm

(d) A=2, B= 1g/250mL, C= 250 rpm

Fig. 1. Preliminary experiment results for color and COD removal.

removal (98%) was reached at pH 2, 1 mg/250 mL catalyst concentration, 250-rpm stirring speed, 60-minute reaction time under the following conditions: a temperature of 25℃, 100 ppm initial dye concentration, and 0.5 mM H_2O_2 concentration.

High temperature more than 25℃ (room temperature) was not preferred because of its high cost in macroscale. According to the preliminary experiments, initial dye concentration was determined as 100 ppm to measure COD accurately. Finally, high H_2O_2 concentration more than 0.5 mM causes interference with COD.

3.2. Experimental design and modeling

To evaluate the influence of operating parameters on color and COD removal efficiency of BB contaminated wastewater, four different factors were chosen for the analysis: pH of the reaction (A), catalyst concentration (B), stirring speed (C), and reaction time (D). After the preliminary experiments, 2^4 full-factorial designs with center points (20 experiments) were employed for the optimization of color and COD removals as response variables. According to the analysis of variance results, the impact of the curvature effect was found to be significant. This means that some of the factors have quadratic effect on the color and COD removals. Secondly, CCD, which is a commonly used design type in RSM, was employed to estimate the response and the coefficients (main effects, interactions, and high-order effects) of the regression model. A total of 28 experiments were run, including 2^4 (16) cube points, 8 axial points, and 4 replications at the center point. Experimental data were analyzed using Design Expert software from Stat Ease Inc., USA. The levels and ranges of factors are given in Table 2.

After performing the experiments randomly, according to the CCD matrix, the coefficients of the model are determined to predict the responses. If the experimental results are fitted to the empirical quadratic polynomial model, this model can be presented as Eq. (7) for which all the coefficients are considered significant according to the ANOVA results.

$$Y = \beta_0 + \beta_1 A + \beta_2 B + \beta_3 C + \beta_4 D + \beta_{11} A^2 + \beta_{22} B^2 + \beta_{33} C^2 + \beta_{44} D^2 + \beta_{12} AB + \beta_{13} AC + \beta_{14} AD + \beta_{23} BC + \beta_{24} BD + \beta_{34} CD \quad (7)$$

where Y represents the response variable (% color or % COD removal), β_0 is the intercept, β_i are the coefficients of the independent variables (A, B, C, D), β_{ii} are the coefficients of quadratic terms, and β_{ij} are the coefficients of the interaction terms.

Table 2
Coded variable levels of the factors

Coded variable levels					
Factors	−1.5(α)	−1	0	1	1.5(α)
PH of the reaction (*A*)	1	2	4	6	7
Catalyst concentration (*B*) g/250 mL	0	0.2	0.6	1	1.2
Stirring speed (*C*) rpm	125	150	200	250	275
Reaction time (*D*) min.	0	10	35	60	72.5

3.3. Statistical Analysis

Following the CCD matrix and experimental results given in Table 3, two quadratic polynomial equations were developed for each response in terms of coded variables as shown in Eqs. (8) and (9). Y_1 and Y_2 represent % color and % COD removals, respectively.

$$Y_1 = 18.53 - 29.175A + 4.498B + 1.26C + 8.224D - 5.251AD + 22.705A^2 + 5.523C^2 \tag{8}$$

$$Y_2 = 18.78 - 17.20A + 6.44B + 3C + 4.41D - 3.38AB - 3AC + 12.03A^2 + 6.25C^2 \tag{9}$$

Table 3
CCD experiments with actual and predicted values of color and COD removals

					Color removal		COD removal	
Run	*A*	*B*	*C*	*D*	Actual	Predicted	Actual	Predicted
1	0	0	−1.5	0	17.84	29.067	29	28.343
2	−1	1	−1	−1	68.63	65.698	55	53.670
3	0	0	0	1.5	27.32	30.860	26	25.395
4	1.5	0	0	0	95.83	113.374	68	71.648
5	0	0	0	0	19.77	18.530	20	18.780
6	1	1	1	1	30.68	26.308	30	27.330
7	0	−1.5	0	0	2.12	11.783	4	9.120
8	−1	−1	−1	1	90.53	83.644	42	42.850
9	0	0	0	0	20.98	18.530	20	18.780
10	1.5	0	0	0	18.57	25.849	17	20.048
11	0	0	0	−1.5	0	6.200	0	12.165
12	1	1	−1	−1	17.95	17.850	17	18.510
13	−1	1	1	1	97.35	95.160	72	74.490
14	−1	−1	−1	−1	57.87	56.702	35	34.030
15	−1	1	1	−1	80.98	68.218	68	65.670
16	1	−1	−1	−1	16.13	8.854	17	12.390
17	0	0	0	0	25.53	18.530	24	18.780
18	1	−1	1	−1	14.31	11.374	18	12.390
19	0	0	1.5	0	19.24	32.847	30	37.343
20	−1	−1	1	−1	61.28	59.222	50	46.030
21	1	−1	1	1	15.83	17.312	20	21.210
22	1	1	1	−1	21.28	20.370	18	18.510
23	1	1	−1	1	27.65	23.788	27	27.330
24	−1	−1	1	1	92.12	86.164	58	54.850
25	0	1.5	0	0	21.28	25.277	32	28.440
26	−1	1	−1	1	94.31	92.640	62	62.490
27	1	−1	−1	1	17.04	14.792	19	21.210
28	0	0	0	0	25.83	18.530	23	18.780

Table 4
ANOVA results of the quadratic model for color removal

Source	Sum of squares	df	Mean square	*F*-value	*p*-value
Model	26,086.31	7	3,726.62	56.50	<0.0001
Residual	1,319.08	20	65.95		
Lack of fit	1,290.16	17	75.89	7.87	0.0572
Pure error	28.12	3	9.64		
Total	27,405.40	27			
	$R^2 = 0.9519$	Adj $R^2 = 0.9350$	Pre. $R^2 = 0.8833$		

Table 5
ANOVA results of the quadratic model for COD removal

Source	Sum of squares	df	Mean square	*F*-value	*p*-value
Model	9,995.14	8	1,249.39	54.83	<0.0001
Residual	432.97	19	22.79		
Lack of fit	420.22	16	26.26	6.18	0.0795
Pure error	12.75	3	4.25		
Total	10,428.11	27			
	$R^2 = 0.9585$	Adj $R^2 = 0.9410$	Pre. $R^2 = 0.9139$		

The experimental data for both color and COD removals were statistically analyzed with the help of ANOVA, and the results are shown in Tables 4 and 5.

As seen in Tables 4 and 5, the ANOVA results of both quadratic polynomial models show that the models are significant according to the *F*-values. *F*-values for the quadratic models are 56.5 and 54.83, respectively, and the *p* values are <0.0001. This means that there is only a 0.01% chance of occurrence of the modeled *F*-values due to noise. On the other hand, the lack of fit means that *F*-values of 7.87 and 6.18 are not significant, with *p* values >0.05. The lack of fit should be insignificant to use this model to make predictions. The ANOVA results for the coefficients of regression models for color and COD removals are shown in Tables 6 and 7, respectively.

R^2 (the coefficient of determination) is defined as the ratio of the explained variation to the total variation and is used as a measure of degree of fit of the model. The predicted R^2 values of 0.9519 and 0.9585 for color and COD removals are in good agreement with the corresponding adjusted R^2 values of 0.9350 and 0.941. For fitting to the experimental data better, the R^2 value should be close to 1. Smaller the value of R^2, lesser will be the fit of the model to the experimental data. The values of R^2 found out indicate that the

Table 6
ANOVA results for the coefficients of quadratic model for color removal

				95% confidence interval			
Factor intercept	Coefficient	df	Std error	Low	High	*F*-value	*p*-value
	18.53	1	2.86	12.55	24.5	–	–
A	−29.175	1	1.794	−32.917	−25.434	264.568	<0.0001
B	4.998	1	1.794	1.257	8.740	7.764	0.0114
C	1.260	1	1.794	−2.482	5.001	0.493	0.4906
D	8.224	1	1.807	4.456	11.992	20.724	0.0002
AD	−5.251	1	2.030	−9.486	−1.016	6.690	0.0176
A^2	22.705	1	2.446	17.604	27.807	86.196	< 0.0001
C^2	5.523	1	2.446	0.422	10.624	5.100	0.0353

Table 7
ANOVA results for the coefficients of quadratic model for COD removal

Factor intercept	Coefficient	df	Std error	95% confidence interval		*F*-value	*p*-value
				Low	High		
	18.78	1	1.68	15.26	22.30	–	–
A	−17.20	1	1.05	−19.40	−14.99	265.99	< 0.0001
B	6.44	1	1.05	4.23	8.65	37.30	< 0.0001
C	3.00	1	1.05	0.79	5.21	8.10	0.0103
D	4.41	1	1.06	2.19	6.63	17.25	0.0005
AB	−3.38	1	1.19	−5.87	−0.88	8.00	0.0107
AC	−3.00	1	1.19	−5.50	−0.50	6.32	0.0211
A^2	12.03	1	1.44	9.02	15.04	70.02	< 0.0001
C^2	6.25	1	1.44	3.24	9.26	18.91	0.0003

quadratic polynomial equations can be used to predict the color and COD removals in the experimental range [11]. Additionally, predicted and adjusted R^2 values for color and COD removals are in good agreement. The actual and predicted values for color and COD removals are given in Table 3.

In the case of color removal, the independent variables *A*, *B*, *D*, the interaction between *A* and *D* (*AD*), and the quadratic terms A^2 and C^2 are highly significant ($p < 0.05$). Although *C* is not significant, its quadratic effect is highly significant, so *C* and C^2 were included to the model together. The main effects of independent factors can be investigated by the help of plots, as in Fig. 2. According to the Fig. 2(a), A has a negative effect on color removal. In other words, color removal has a maximum value when the *A* (pH) is 2.

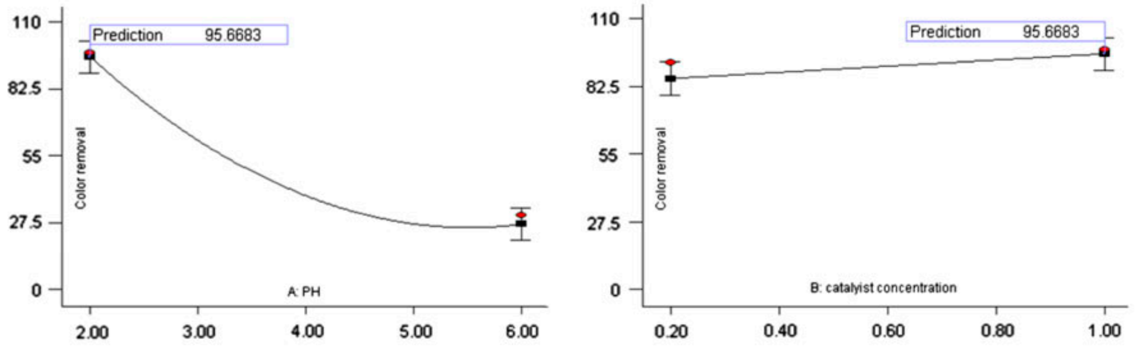

(a) B=1 g/250 mL C=250 rpm D=60 min. **(b)** A=2 C=250 rpm. D=60 min.

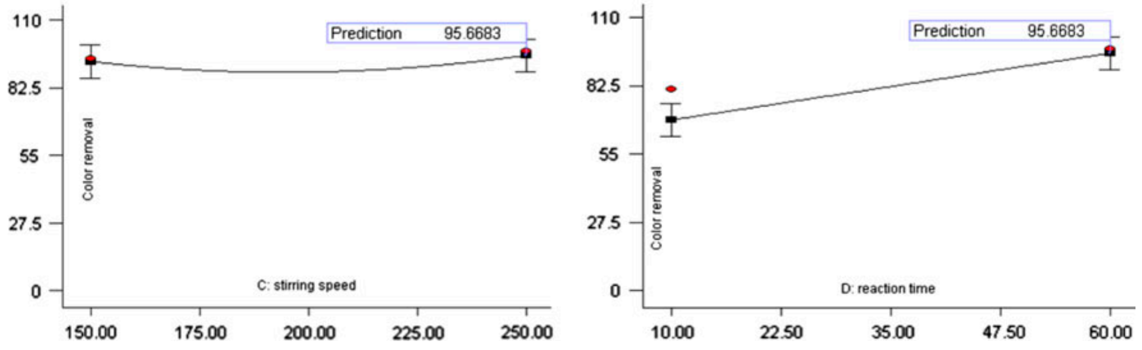

(c) A=2 B=1 g/250 mL D=60 min. **(d)** A=2 B=1 g/250 mL C=250 rpm

Fig. 2. The main effect plots for color removal.

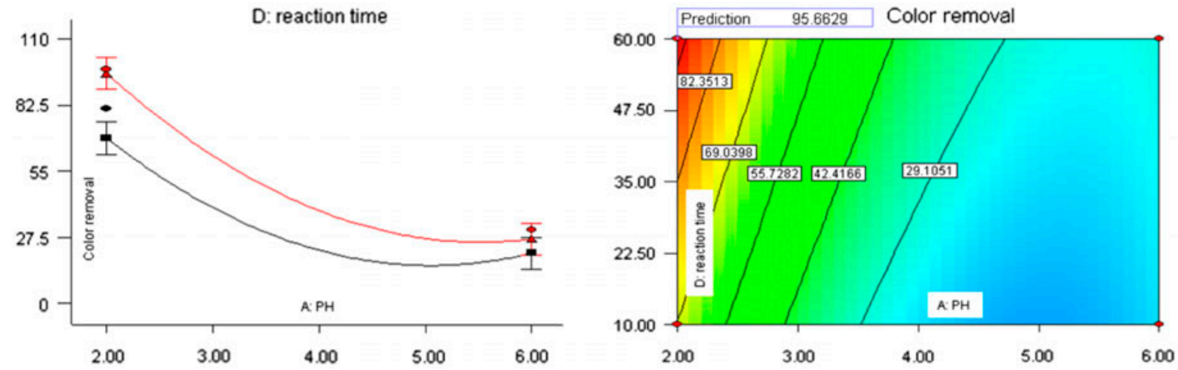

Fig. 3. AD interaction effect for color removal (*B* = 1 g/250 mL *C* = 250 rpm).

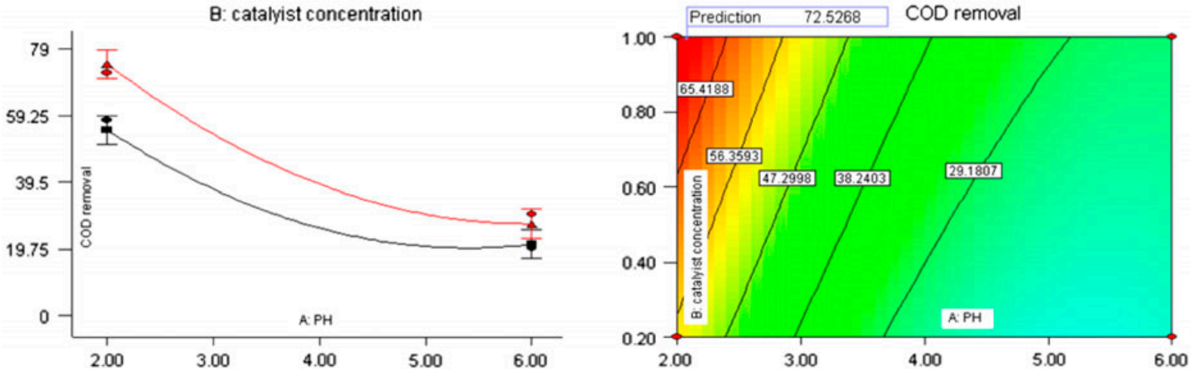

Fig. 4. *AB* interaction effect for COD removal (*C* = 250 rpm *D* = 60 min.).

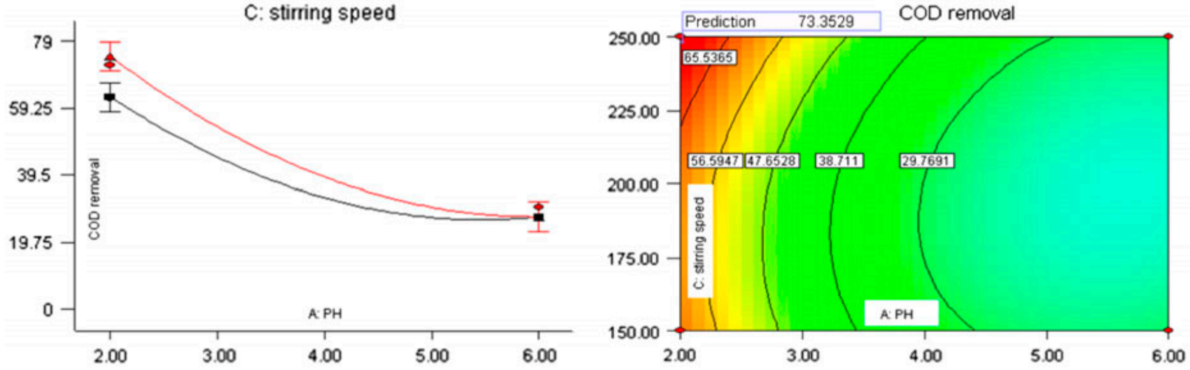

Fig. 5. *AC* interaction effect for COD removal (*B* = 1 g/250 mL *D* = 60 min.).

On the other hand *B*, *C*, and *D* have a positive effect on color removal (Fig. 2(b)–(d)). The quadratic effects of *A* and *C* are also seen by the related curves in Fig. 2(a) and (c) easily. Fig. 3 shows that color removal has a maximum value when the pH is 2 and reaction time is 60 min.

The main effect plots for the COD removal are similar to color removal. *A* has a negative effect on COD removal, while the other factors have positive effects on it. *A* has a quadratic effects on COD removal similar to *C*. *AB* and *AC* interaction effects for COD removal are shown in Figs. 4 and 5.

According to the Figs. 4 and 5, example prediction points from the red area show that COD removal reaches its maximum value when the pH is on the lower bounds (2) catalyst concentration and stirring

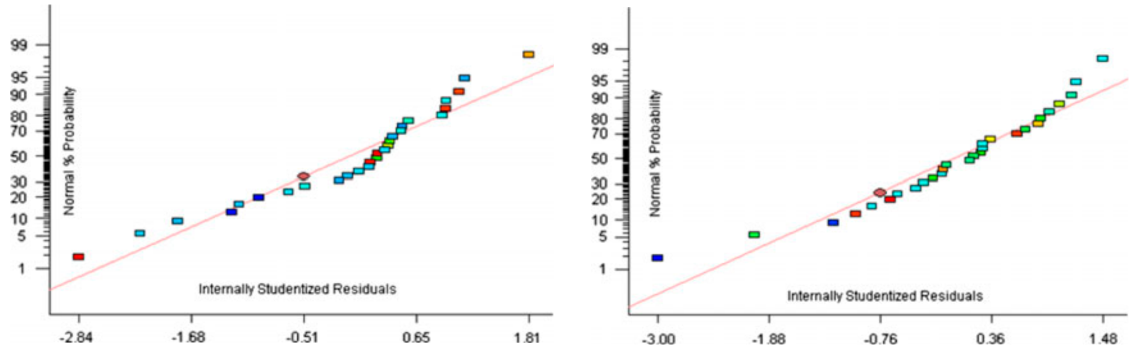

(a) Color Removal **(b)** COD Removal

Fig. 6. Normal probability plots of internally studentized residuals.

speed are on the upper bounds (1 g/250 mL and 250 rpm).

Normal probability plots of internally studentized residuals is an important diagnostic tool for detecting the systematic departures from the assumption that errors are normally distributed and they are independent of each other [11]. The normal probability plots of residuals for color and COD removals are shown in Fig. 6(a) and (b). This figure confirms the normality assumptions and independence of the residuals for color and COD removals.

3.4. Simultaneous optimization

The most popular approach to simultaneous response optimization is the desirability function approach, as proposed by Derringer and Suich [17]. Individual goals are combined into an overall desirability function to find the local solutions.

The desirability procedure involves two steps. In the first step, the levels of the independent variables that simultaneously produce the most desirable predicted responses of the dependent variables are found. In the second step, overall desirability is maximized with respect to the controllable factors. Therefore, desirability functions are used to obtain qualitative and quantitative responses by the simple and quick transformation of different responses to one measurement. Generally speaking, the first step when using desirability functions is to convert each response into an individual desirability function (d_i), the values of which vary from 0 to 1 (lowest desirability to highest desirability).

The individual desirability scores for the predicted values of each dependent variable are then combined in an overall desirability function, D, by computing the geometric mean of different d_i values as shown in Eq. (10):

$$D = [d_1 \times d_2 \times \cdots \times d_n]^{1/n} \tag{10}$$

where d_{i} indicates the desirability of response i and n is the number of responses in the measure. If any of the responses do not satisfy their desirability requirement(s), the overall function becomes zero. Formulation can be extended to

Table 8
Local solution sets with desirability values

Solutions	pH	Catalyst C.	Stirring S.	Reaction time	Color removal	COD removal	Desirability
1***	2	1.000	249.630	60.000	95.524	74.313	0.991
2	2	0.850	249.700	60.000	93.723	70.704	0.972
3	2	0.990	239.510	60.000	93.260	70.746	0.970
4	2	1.000	245.360	52.860	90.720	71.555	0.962
5	2	1.000	250.000	50.990	90.135	72.478	0.962
6	2	1.000	249.930	48.390	89.386	72.404	0.958
7	2	1.000	250.000	47.820	89.096	72.329	0.957
8	2	1.000	233.430	60.000	92.190	69.031	0.953
9	2	0.770	250.000	60.000	91.502	68.122	0.943
10	2	0.610	250.000	60.000	90.777	64.885	0.917

Note: ***selected solution.

Table 9
Results of the confirmation

Response	Prediction	95% PI low	95% PI high	Confirmatory trial
% Color removal	95.524	76.177	114.871	96
% COD removal	74.313	62.636	85.990	75

$$D = [d_1^{\alpha_1} \times d_2^{\alpha_2} \times \cdots \times d_n^{\alpha_n}]^1/n, \quad 0 \le \alpha_i \le 1$$
$$i = (1, 2, 3, \cdots, n) \quad \alpha_1 + \alpha_2 + \cdots + \alpha_n = 1 \tag{11}$$

where d_i indicates the desirability of the different responses Y_i ($i = 1,2,3, \ldots, n$) and α_i represents the relative importance of the individual responses. Thus, the maximum overall desirability function, D, depends on the importance values.

For the simultaneous optimization of color and COD removal, the optimization function in the Design Expert software was used. Optimization was carried out by generating a global desirability function (D) that assigned a value ranging from 0 to 1 to each solution (see Table 8).

The first highlighted solution is selected with the highest desirability value of 0.991. According to the first solution, optimized reaction conditions were established as a pH of 2, 1 g/250 mL catalyst dose, 250 rpm stirring speed and a 60 min reaction time. Estimated % removals of color and COD are 95.524 and 74.313, respectively.

4. Confirmation

A useful measure of confirmation is to ensure that the predicted responses fall within the PI for each response at the optimal point [18]. A 100(1−α) percent PI for the future observation y_0 at point x_0 is:

$$\hat{y}(x_0) - t_{\alpha/2,n-p}\sqrt{\hat{\sigma}^2(1 + x_0'(X'X)^{-1}x_0)} \le y_0 \le \hat{y}(x_0) + t_{\alpha/2,n-p}\sqrt{\hat{\sigma}^2(1 + x_0'(X'X)^{-1}x_0)} \tag{12}$$

where $\hat{y}(x_0) = x_0'\hat{\beta}$ is the model prediction for the future observation, n is the number of observations in the original experiment, p is the number of coefficients in the model developed from the original experiment, $t_{\alpha/2\ n-p}$ is the upper $\alpha/2$ percentage point of the t distribution with n-p degrees of freedom, and $\hat{\sigma}^2$ = MSE. Validation of the PI is performed by predicting the response at a selected point using the developed model, calculating the PI, and then conducting a confirmation experiment at that selected point to measure the new response [14].

For the optimized reaction conditions, an additional experiment was carried out under the same conditions as the original experiment. Percent removals of color and COD were measured for the confirmation, and the results are shown in the last column of Table 9. According to the confirmatory trial, 96% color and 75% COD removals fell within the PI with a 95% confidence level. The results verify that the model predicts the optimal point well.

5. Conclusion

In this study, RSM and CDD was successfully employed to optimize the levels of operational parameters such as pH of the reaction, catalyst concentration, stirring speed, and reaction time on the heterogeneous Fenton-type oxidation of BB. The study was conducted by Fe (III) sepiolite catalyst in the presence of hydrogen peroxide (H_2O_2) in a batch process. From the quadratic models developed for the color removal and subsequent ANOVA test using the Design Expert trial version, the influential factors such as pH of the reaction, catalyst concentration, reaction time, interaction between pH, and reaction time and the quadratic effects of pH and stirring speed are highly significant. The models fitted very well to the experimental data as confirmed by the high R^2, adjusted R^2, and predicted R^2 values. According to the ANOVA results of COD removal, individual effects of all the factors and quadratic effects of pH and stirring speed are significant. Interaction effects of pH and catalyst concentration, and pH and stirring speed are also significant. For the simultaneous optimization of color and COD removals, desirability functions were used and optimized reaction conditions were established as a pH of 2, 1 g/250 mL catalyst dose, 250-rpm stirring speed, and a 60-min reaction time. Under the optimum conditions, color and COD removal were predicted to be 95.524 and 74.313%, respectively, and the corresponding confirmatory trial values (96% and 74%) fit well to the dataset of predicted values.

Acknowledgements

This paper is a part of the results of project number 201215D13 funded by Eskisehir Osmangazi University. The authors wish to thank their university for all the support provided.

References

[1] R. Idel-aouad, M. Valiente, A. Yaacoubi, B. Tanouti, M.L. López-Mesas, Rapid decolorization and mineralization of the azo dye C.I. Acid Red 14 by heterogeneous Fenton reaction, J. Hazard Mater. 186 (2011) 745–750.

[2] F. Martínez, G. Calleja, J.A. Melero, R. Molina, Heterogeneous photo-Fenton degradation of phenolic aqueous solutions over iron-containing SBA-15 catalyst, Appl. Catal., B 60 (2005) 181–190.

[3] Y. Aşçı, Decolorization of Direct Orange 26 by heterogeneous fenton oxidation, Desalin. Water Treat. 51(40-42) (2013) 7612–7620.

[4] M.B. Kasiri, A.R. Khataee, Photooxidative decolorization of two organic dyes with different chemical structures by UV/H_2O_2 process: Experimental design, Desalination 270 (2011) 151–159.

[5] I. Arslan-Alaton, G. Tureli, T. Olmez-Hanci, Treatment of azo dye production wastewaters using Photo-Fenton-like advanced oxidation processes: Optimization by response surface methodology, J. Photochem. Photobiol., A 202 (2009) 142–153.

[6] C.S.D. Rodrigues, L.M. Madeira, R.A. Boaventura, Optimization of the azo dye Procion Red H-EXL degradation by Fenton's reagent using experimental design, J. Hazard. Mater. 164 (2009) 987–994.

[7] M. Azami, M. Bahram, S. Nouri, A. Naseri, A central composite design for the optimization of the removal of the azo dye, methyl orange, from waste water using the Fenton reaction, J. Serb. Chem. Soc. 77–2 (2011) 235–246.

[8] H.Y. Xu, S.Y. Qi, Y. Li, Y. Zhao, J.W. Li, Heterogeneous Fenton-like discoloration of Rhodamine B using natural schorl as catalyst: Optimization by response surface methodology, Environ. Sci. Pollut. Res. 20 (2013) 5764–5772.

[9] F. Ay, E.C. Catalkaya, F. Kargi, A statistical experiment design approach for advanced oxidation of Direct Red azo-dye by photo-Fenton treatment, J. Hazard. Mater. 162 (2009) 230–236.

[10] N. Masomboon, C.W. Chen, J. Anotai, M.C. Lu, A statistical experimental design to determine o-toluidine degradation by the photo-Fenton process, Chem. Eng. J. 159 (2010) 116–122.

[11] C. Sahoo, A.K. Gupta, Optimization of photocatalytic degradation of methyl blue using silver ion doped titanium dioxide by combination of experimental design and response surface approach, J. Hazard. Mater. 215-216 (2012) 302–310.

[12] M. Dopar, H. Kusic, N. Koprivanac, Treatment of simulated industrial wastewater by photo-Fenton process. Part I: The optimization of process parameters using design of experiments (DOE), Chem. Eng. J. 173 (2011) 267–279.

[13] W. Li, C. Su, Modeling and optimization of acid chrome dark blue degradation by fenton using box-behnken response surface methodology, IEEE, ISBN:978-1-4244-9439-2 (2011), 7463–7466, doi: 10.1109/MACE.2011.5988776.

[14] I. Grčić, D. Vujević, N. Koprivanac, The use of D-optimal design to model the effects of process parameters on mineralization and discoloration kinetics of Fenton-type oxidation, Chem. Eng. J. 157 (2010) 408–419.

[15] H.Y. Xu, X.L. He, Z. Wu, L.W. Shan, W.D. Zhang, Iron-loaded natural clay as heterogenous catalyst for fenton-like discoloration of dyeing wastewater, Bull. Korean Chem. Soc. 30–10 (2009) 2249–2252.

[16] H.Y. Xu, M. Prasad, Y. Liu, Schorl: A novel catalyst in mineral-catalyzed Fenton-like system for dyeing wastewater discoloration, J. Hazard. Mater. 165 (2009) 1186–1192.

[17] G. Derringer, R. Suich, Simultaneous Optimization of Several Response Variables, J. Qual. Tech. 12 (1980) 214–219.

[18] D.C. Montgomery, Design and Analysis of Experiments, sixth ed., John Wiley & Sons, New York, NY, 2005.